New Developments in Understanding the Chemistry of Cement Hydration [and Discussion]

D. D. Double, P. C. Hewlett, K. S. W. Sing and J. F. Raffle

Phil. Trans. R. Soc. Lond. A 1983 **310**, 53-66
doi: 10.1098/rsta.1983.0065

Phil. Trans. R. Soc. Lond. A **310**, 53–66 (1983) [53]
Printed in Great Britain

New developments in understanding the chemistry of cement hydration

By D. D. Double
Department of Metallurgy and Science of Materials,
University of Oxford, England, U.K.

[Plate 1]

Portland cement is based on calcium silicates with lesser amounts of calcium aluminates. Its reaction with water, which is responsible for strength development, is a complex process involving the precipitation of hydration products in colloidal gel and crystalline forms. This paper describes the microstructural development of the hydrates the structure of colloidal C–S–H gel, which is the main hydration product, the kinetics of hydration and the aqueous solution chemistry of cement pastes and pastes made with pure C_3S. Theories relating to the mechanism of cement hydration are examined and these are discussed in terms of studies of the effect of accelerating and retarding admixtures for cement.

1. Anhydrous cement constituents and hydration products

Portland cement sets and hardens by chemical reaction with water. The development of strength of a cement paste is associated with the precipitation of hydration products of very low solubility to form a cohesive matrix binding the residual cement grains into a composite solid.

The main constituents of anhydrous cement clinker are slightly impure forms of tricalcium silicate (C_3S, about 50 % by mass), dicalcium silicate (C_2S, *ca.* 25 %), tricalcium aluminate (C_3A, *ca.* 10 %) and an aluminoferrite phase approximating to the formula C_4AF (*ca.* 10 %). The hydration chemistry is dominated by the calcium silicate phases and these provide the main source of strength development in a cement paste. The aluminate phases, in particular C_3A, affect the setting behaviour but are not thought to contribute significantly to the overall strength attainment. The C_3S phase hydrates faster than C_2S and since it is also the major constituent in Portand cement it is often taken as the model system by experimentalists in studying cement chemistry.

A summarized scheme of the hydration process is shown in figure 1, illustrating the anhydrous constituents in relation to their hydration products. In spite of their difference in reactivity, the hydration products of C_3S and C_2S are essentially the same. The main product is calcium silicate hydrate (C–S–H) gel, a colloidal precipitate, which is mainly amorphous and which has a rather variable composition. This occupies about 60 % (by volume) of the hydration products and is therefore the main binding agent in hardened cement. Calcium hydroxide is a by-product of the hydration of the calcium silicates and contributes a further 20 % (by volume) approximately. The rest comprises various calcium sulphoaluminate and aluminoferrite hydrates, which are the products of hydration of the aluminate phases and gypsum. Gypsum (*ca.* 2 %) is deliberately added to Portland cement to control the rapid hydration of C_3A, which otherwise tends to produce premature 'flash setting' of the cement. Apart from calcium hydroxide, crystalline products of hydration detectable by X-ray diffraction include ettringite ($C_3A.3C\bar{S}.32H$) and calcium monosulphoaluminate ($C_3A.C\bar{S}.12H$).

The reactions shown in figure 1 do not occur independently and there is appreciable fine-scale mixing of the hydrates, particularly in the colloidal gel product. During hydration, there is an increase in the volume of solids and this is accommodated by growth of the hydrates into the water filled spaces in the cement microstructure during the hardening process.

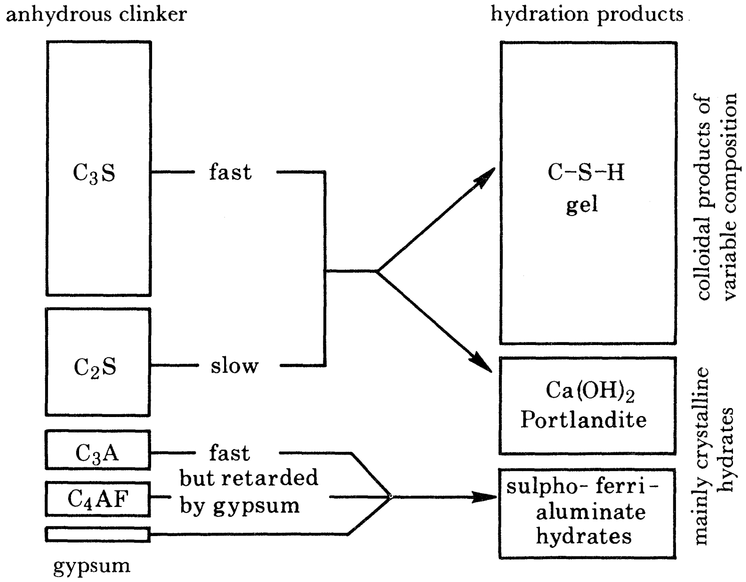

Figure 1. Schematic representation of the anhydrous constituents in Portland cement clinker and the products formed during hydration. The areas of the 'boxes' give the approximate volume proportions of the phases.

2. Development of microstructure during hydration

Electron microscopy has been widely used to study the formation of hydration products in cements and in samples made from pure cement compounds (Daimon *et al.* 1971; Williamson 1972; Collepardi & Marchese 1972; Lawrence & Young 1973; Diamond 1976). The main features of a hydrated cement are shown in figure 2 (plate 1). On the fractured section, the prominent morphology is a reticular structure consisting of irregular fibres growing from the surfaces of the cement grains and bridging the spaces between. This material is identified as the C–S–H gel hydration product. Large plate-like crystals of calcium hydroxide also occur in the microstructure. Similar microstructures occur in hydrated samples of pure C_3S and C_2S. The development of C–S–H gel growths in a sample of C_3S at early stages of hydration is shown in figure 3 (plate 1). In mature, fully aged cements there is much infilling and consolidation of the microstructure by fine grained C–S–H gel and by growth of crystalline hydration products. In general, the morphology of C–S–H gel is variable depending on the w/c ratio and age of the cement sample, so it is difficult to classify characteristic types.

The growth of hydration products at the surfaces of cement grains has been studied in detail by transmission electron microscopy methods (Double *et al.* 1978; Jennings & Pratt 1979; Groves 1981). These show essentially a two-stage process. On contact with water, the cement grains almost immediately become enveloped by thin coatings of colloidal gelatinous hydrates. The coatings are of the order 0.1–1.0 μm in thickness and give only weak diffuse diffraction rings against the spot patterns emanating from the underlying crystalline clinker mineral (figure 4, plate 1). At later stages, after several hours, secondary growth of C–S–H gel occurs,

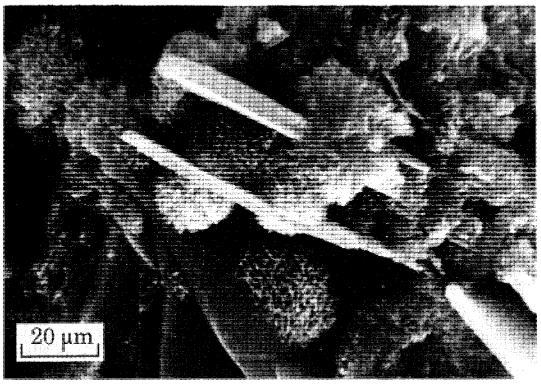

FIGURE 2. Fracture surface of a hardened cement paste showing fibrillar growth of C–S–H gel around the cement grains and plate-like crystals of calcium hydroxide (w/c ratio 0.7, age 40 days). Scanning electron micrograph.

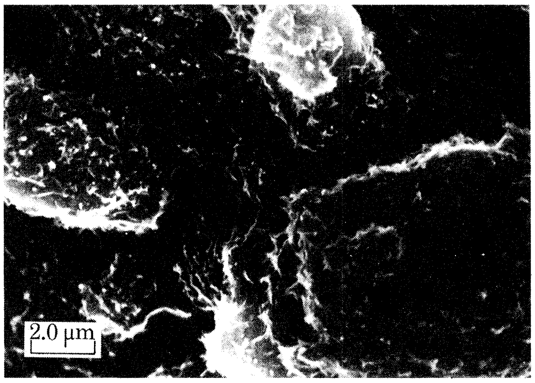

FIGURE 3. Fracture surface of a C_3S paste sample at early stages of hydration showing gel coatings around the particles and the beginning of the growth of fibrillar C–S–H gel product (w/c ratio 0.5, age 2 h). Scanning electron micrograph.

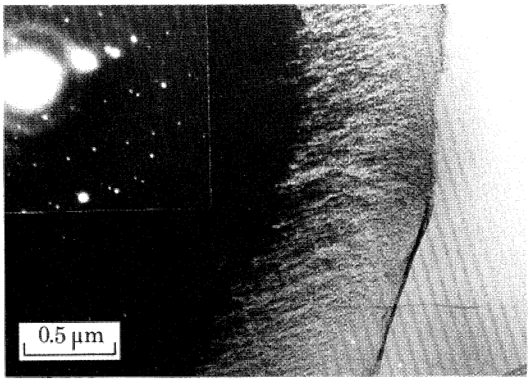

FIGURE 4. Colloidal gel coating formed on a grain of C_3S in a thinned slice of Portland cement clinker after dipping in water for 5 min. Transmission electron micrograph and selected area diffraction pattern (Groves 1981).

FIGURE 5. Secondary growth of C–S–H gel at the surfaces of cement grains after hydration for 21 h, the hydrate shows fibrillar and crumpled sheet type morphologies. Transmission electron micrograph.

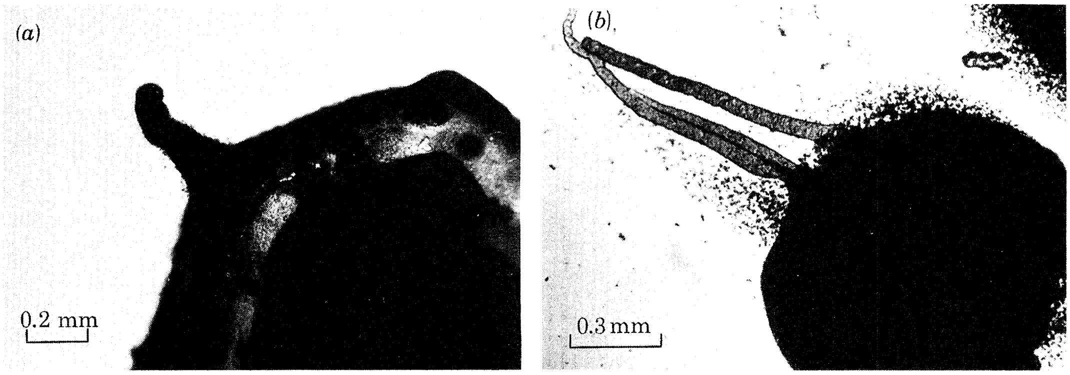

FIGURE 10. 'Silicate garden' obtained by immersing a grain of sodium silicate in dilute aqueous calcium nitrate solution. (*a*) Formation of colloidal C–S–H gel coating around the dissolving grain. (*b*) Tubular growths formed after osmotic rupture of the gel coating. Optical micrographs.

sometimes in fibrillar form and sometimes as exfoliated crumpled sheets (figure 5, plate 1). As in s.e.m. observations, t.e.m. studies show a variety of morphological forms of C–S–H gel. The observation that the fibrillar growths sometimes show hollow tubular structures (Double *et al.* 1978) is interesting, since it relates to theories of the mechanism of cement hydration. Analysis of the fibres gives compositions that include appreciable amounts of aluminium and sulphur in addition to calcium and silicate (Jennings & Pratt 1979). Amorphous tubular growths have also been reported in studies of C_3A hydrated in lime with gypsum solutions, the fibres having C–A–$\bar{S}$–H type compositions (Bailey & Chescoe 1976).

A distinction is often made, in terms of composition and structure, between 'inner' and 'outer' hydration products. This differentiates between those products precipitated within the original outline of the cement grain as it dissolves during hydration and those growing in the water-filled spaces outside. The microstructures described above constitute outer products. Inner products, adjacent to the cement grain surface, usually have a very fine grained and compact texture.

3. COMPOSITION AND STRUCTURE OF C–S–H GEL

Electron microscopy shows that the basic structure of C–S–H gel is an agglomeration of colloidal particles of rather indefinite shape but generally less than 50 nm size. This is consistent with large surface areas and very fine porosity determined by mercury intrusion and gas adsorption techniques (Brunauer *et al* 1967; Diamond 1971) and by X-ray and neutron low-angle scattering methods (Winslow & Diamond 1974; Allen *et al.* 1982). The composition of C–S–H gel is variable and probably depends on locality in the microstructure (namely, inner and outer hydration products) and on the age of the sample. Electron microanalysis studies applied to cement and C_3S samples give CaO/SiO_2 molar ratios in C–S–H gel ranging between 1.5 and 2.0, a notable feature in cement samples being the inclusion of appreciable quantities of Al, Fe, S and alkali impurities (Taylor & Roy 1980). In addition to compositional variations, structural rearrangements occur with time. Trimethylsilylation techniques have been used to study the degree of polymerization of the silicate (Taylor & Roy 1980). The conclusions are that the silicate in C–S–H gel in hydrated cement and C_3S samples is mainly dimeric at early stages of hydration ($Si_2O_7^{6-}$ units), but that there is a progressive condensation to higher polymeric forms (greater than tetramer) with ageing. Even in samples several years old, the dimeric fraction may be as much as a third of the total.

4. CHEMISTRY OF HYDRATION

The reaction between cement compounds and water is exothermic, and calorimetric methods have proved effective in studying the sequence of hydration (Stein 1961; Tenoutasse 1969; Previte 1971; Double *et al.* 1978). Figure 6 shows the general form of the heat evolution curve obtained from a sample of C_3S.

Hydration occurs in a number of distinct stages and these are characterized by an initial very rapid evolution of heat within the first few minutes and a later more gradual peak reaching a maximum after about 8–10 h and decreasing slowly thereafter. The peaks are separated by an 'induction period' lasting between 1 and 3 h, when the rate of heat evolution drops to a very low value. The initial peak is largely due to the heat of wetting of the C_3S powder and the hydration of any free lime in the sample. An increase in temperature accelerates hydration and this is seen in the calorimetric curve as a shortening of the induction period and an increase in height of the second peak, which is brought to an earlier time interval. The same form of heat evolution is shown by cement, although modified by additional contributions from the other constituents, notably by the hydration of C_3A and at later stages by the hydration of C_2S. In terms of the microstructural developments discussed previously, the initial peak corresponds to the formation of gelatinous coatings of hydration products around the cement grains. The later accelerational period corresponds to the beginning of the secondary growth of C–S–H gel hydration products. In practical terms, the accelerational stage is important since it covers the period of setting of the cement paste under normal conditions.

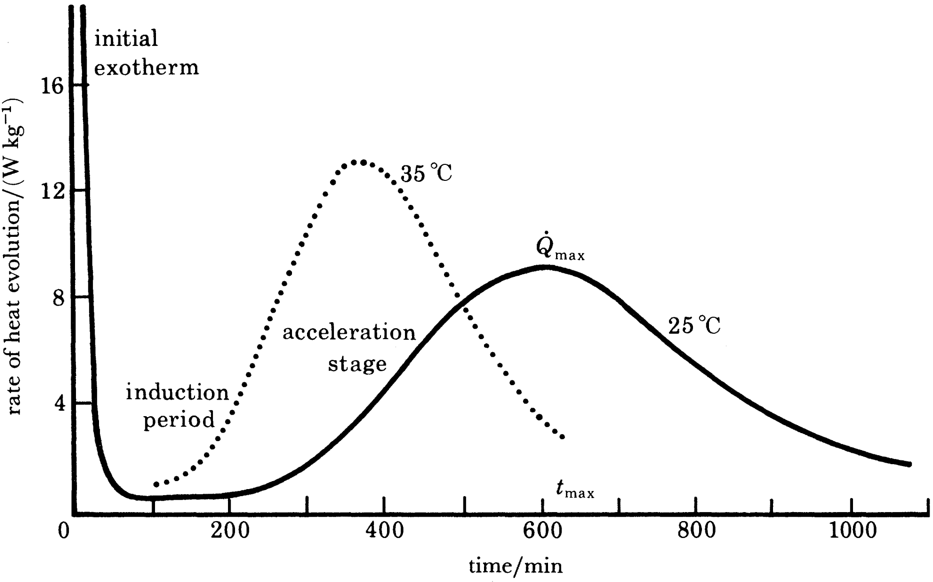

FIGURE 6. General form of the heat evolution curve obtained during the hydration of C_3S. The dotted line shows the accelerating effect of increasing the temperature of hydration.

It is relevant to consider the calorimetric curves in relation to changes in the aqueous solution chemistry of a cement paste. Techniques involve extracting and filtering the liquid phase from a cement or C_3S paste at various stages of hydration and analysing for dissolved species (Lawrence 1966; Tadros *et al.* 1976; Young *et al.* 1977; Barret & Ménétrier 1980; Thomas & Double 1981; Thomas *et al.* 1981). Results tend to vary depending on the methods used, but the curves shown in figure 7*a*, *b* are generally typical.

In the simpler case of a pure C_3S paste (figure 7*a*), there is initially a very rapid rise in the calcium and hydroxyl ion levels within a few minutes of mixing with water. This is followed by a more gradual increase, which reaches a maximum after about 3–5 h. The solubility limit of calcium hydroxide is exceeded within about 20–30 min and the final peak represents a supersaturation by a factor between 1.5 and 2. A significant feature is that during this period the concentration of silicate in solution is almost negligibly small, generally less than $2/10^6$. In relation to the calorimetric curves, two points are worth noting. First, that the calcium and hydroxyl ion concentrations are continuously rising during the induction period. Second, that the supersaturation peak corresponds approximately to the end of the induction period and the stage of accelerated reaction.

In a cement paste (figure 7*b*), the situation is more complex but the underlying features are

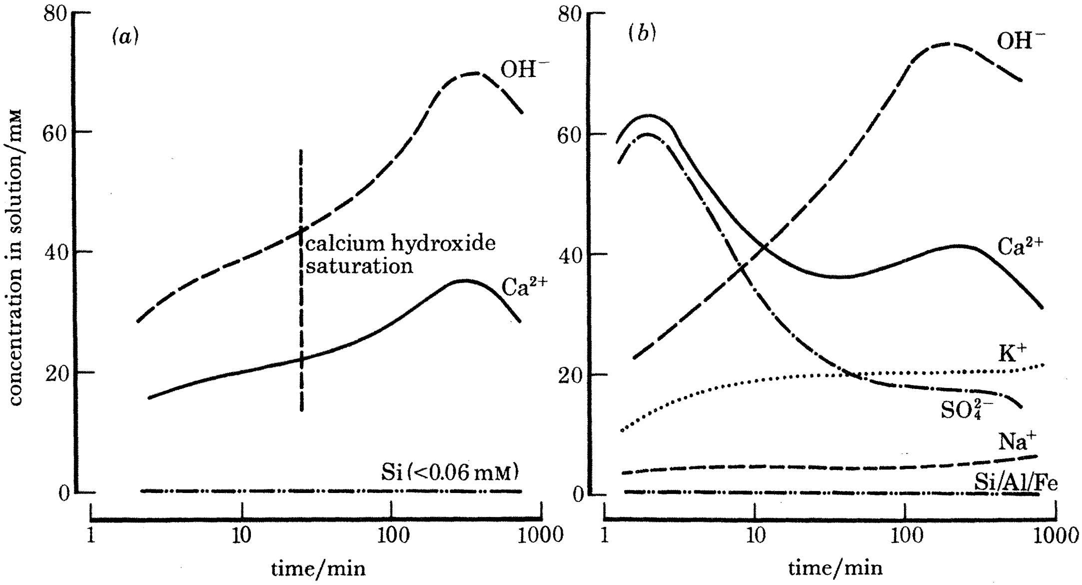

FIGURE 7. Typical concentration against time curves obtained by chemical analysis of solutions filtered from (*a*) a C_3S paste sample and (*b*) Portland cement paste (w/c ratio = 2).

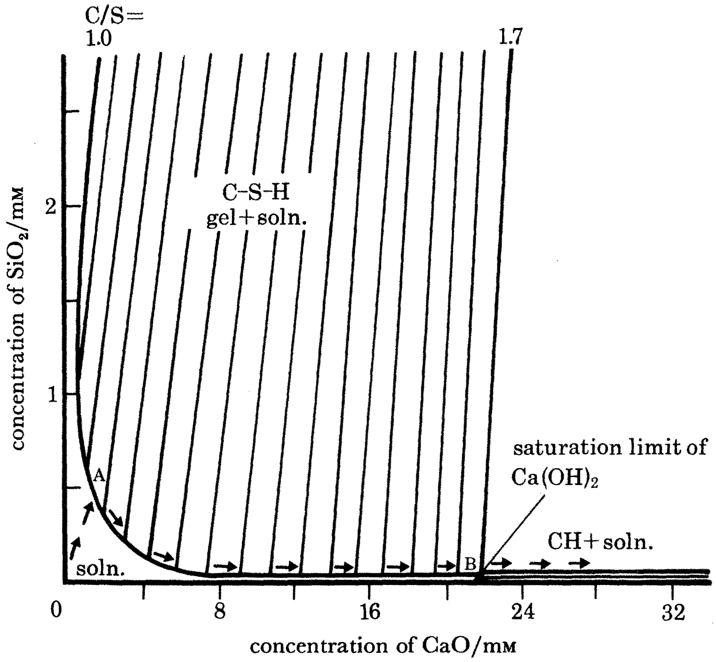

FIGURE 8. General form of the solubility diagram for the ternary $CaO-SiO_2-H_2O$ system at room temperature (based on Flint & Wells 1934). The arrows indicate the expected changes in lime and silica concentrations in solution during the hydration of C_3S.

similar. Solutions show rising concentrations of calcium and hydroxyl ions reaching a supersaturation peak, and silicon concentrations that remain extremely small throughout. Aluminum and iron are also almost absent from solution (*ca.* $2/10^6$ or less). Superimposed on this are increasing concentrations of sodium and potassium from the alkalis in cement and an early peak in the concentrations of calcium and sulphate. The latter may be attributed to the dissolution of gypsum in the cement and its combination with the aluminate phases to precipitate sulphoaluminate hydrates.

The calcium silicon ratios in solution from cement and C_3S pastes are generally in the range $(10^2–10^3):1$. It has been shown that these concentrations may be correlated with data from experimentally determined solubility limits in the ternary $CaO–SiO_2–H_2O$ system (Thomas & Double 1981). The solubility diagram shown in figure 8 is based on the work of Flint & Wells (1934), but is drawn on an exaggerated scale for clarity (the solubility of silica in lime solution is very much smaller than shown, generally less than 0.05 mM).

The solubility diagram illustrates two points. The first is the insolubilization of silica in the presence of lime by precipitation as C–S–H gel. The second is the variability in the CaO/SiO_2 ratio of the C–S–H gel depending on the composition of the solution with which it is in contact (as indicated by the changing slopes of the tie-lines in the two phase C–S–H gel + solution region). Solution compositions in C_3S pastes generally lie along the line AB, the solubility limit of C–S–H gel, with lime concentrations increasing with time. The point B, which is an invariant point where both the solids C–S–H gel + $Ca(OH)_2$ are in equilibrium with saturated solution, is in practice exceeded as the solution approaches the supersaturation peak. Under normal circumstances, the initial hydrolysis of C_3S probably does not involve congruent dissolution. In any case the solubility limit of C–S–H gel is reached very soon after the contact of C_3S with water, and this is associated with the almost immediate precipitation of C–S–H gel at the surfaces of the grains. The rising concentration of lime in solution is a consequence of the precipitation of C–S–H gel with a lower CaO/SiO_2 ratio (ranging between 1.5 and 1.7 according to the solubility diagram) than the surrounding solution.

5. Mechanism of cement hydration

Questions relating to the mechanism of cement hydration are the subject of much debate in the literature (Skalny & Young 1980). The situation is complicated by the possibility that different rate controlling factors may operate at various stages of hydration. As far as early hydration is concerned, one can identify at least three possible rate determining processes: (*a*) the hydrolysis of the anhydrous clinker phases, (*b*) the nucleation and growth of the hydration products and (*c*) the diffusion of water and solute species through coatings of hydration products around the cement grains. That stage (*a*) may be important is indicated by reports that the reactivity of C_3S is influenced by polymorphic modification and by defects introduced by prior grinding or quenching and by u.v. excitation of the clinker (Fierens & Verhaegen 1976; Maycock *et al.* 1978; Aldous 1983).

In general terms, models for cement hydration divide into two categories: 'delayed nucleation theories' and 'protective coating theories'. The former mainly concentrate on the delayed nucleation of calcium hydroxide, associating the end of the induction period with the supersaturation peak in solution (Tadros *et al.* 1976; Young *et al.* 1977; Dent Glasser *et al.* 1978). The nucleation of calcium hydroxide is seen as being poisoned by the adsorption of small amounts of silicate from solution. The increasing concentration of lime in solution is then seen as progressively inhibiting the hydration of the cement silicates (induction period), a situation that is relieved only when $Ca(OH)_2$ eventually nucleates and grows. Evidence contrary to these ideas comes from experiments that show that the hydration of cement or C_3S is not significantly accelerated either by hydrating in already saturated lime solution or by prior 'seeding' of the paste sample by crystalline calcium hydroxide (Odler & Dorr 1979). Also, the presence of crystalline calcium hydroxide has sometimes been detected long before the supersaturation peak and the end of the induction period (Slegers & Rouxhet 1977). Alternative theories that invoke delayed nucleation of C–S–H gel as the rate controlling factor (Fierens & Verhaegen 1976; Odler & Dörr 1979) do not seem compatible with studies of the aqueous solution chemistry or electron microscopy observations that show almost immediate precipitation of C–S–H gel when cement silicate grains contact water.

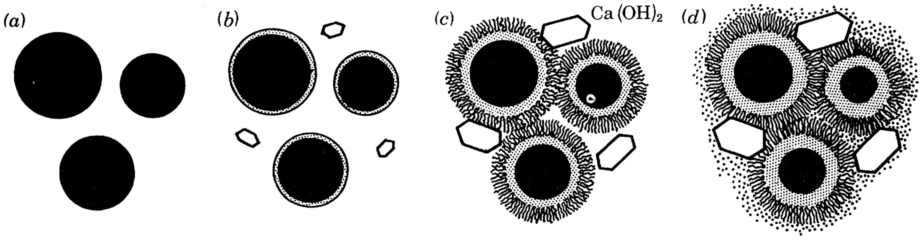

FIGURE 9. Schematic representation of the sequence of hydration of cement. (*a*) Cement grains in water. (*b*) Formation of protective colloidal coatings of C–S–H gel around the cement grains. (*c*) Rupture of the protective coatings followed by secondary growth of C–S–H gel. (*d*) Later infilling of the microstructure by fine grained C–S–H gel and by growth of crystalline calcium hydroxide.

Protective coating theories view the growth of calcium hydroxide as the effect of accelerated hydration rather than the cause. The proposed sequence of events is schematically illustrated in figure 9. The rapid precipitation of C–S–H coatings around the cement grains provides protective barriers that inhibit the access of water and retard hydration during the induction period. The end of the induction period occurs when the coatings are disrupted, thus leading to accelerated hydration and growth of secondary C–S–H gel hydration products. The acceleration period is followed by a gradually decreasing rate of reaction and this is attributed to later infilling and accretion by hydration products. Effectively, as the layers of hydration products thicken by growth around the cement grains and as free water in the microstructure is consumed, longer range diffusional processes dominate and progressively slow down hydration.

The important question is the cause of the disruption of the initial protective coating. One explanation is that there is a spontaneous change in the chemical and physical structure of the C–S–H gel, a transition to a secondary C–S–H hydrate that is more permeable to the diffusion of water and solute species (de Jong *et al.* 1967). There is no direct experimental evidence, however, that such a phase change occurs in C–S–H gel within the induction period. An alternative proposal, based on an original suggestion by Powers (1961), is that the coatings are ruptured by osmotic pressure effects due to the selectively permeable character of the colloidal gel. This is the basis of the 'osmotic membrane' model for cement hydration (Double *et al.* 1978, 1980; Birchall *et al.* 1978, 1980). In this model the C–S–H gel coating is seen as acting as a membrane that allows inward diffusion of water to the cement grains and outward diffusion of calcium and hydroxyl ions released by hydrolysis. The membrane is, however, effectively impermeable to the outward diffusion of the larger and sterically hindered silicate ions. Preferential diffusion leads to a rising osmotic pressure within the coating sufficient eventually at the end of the induction period, to cause its rupture and exfoliation. The hydrous silicate, originally retained within the membrane coating, is extruded into outer lime-rich bulk solution where it is immediately precipitated as secondary C–S–H gel products growing from the surfaces of the original coating. The model explains the transport of solute species during hydration and precipitation (calcium and hydroxyl ion concentrations rising during the induction period, yet negligible quantities of silicate in the bulk solution) and is also consistent with the observed morphological development of the secondary C–S–H gel hydration products (in fibrillar, crumpled sheet and tubular forms).

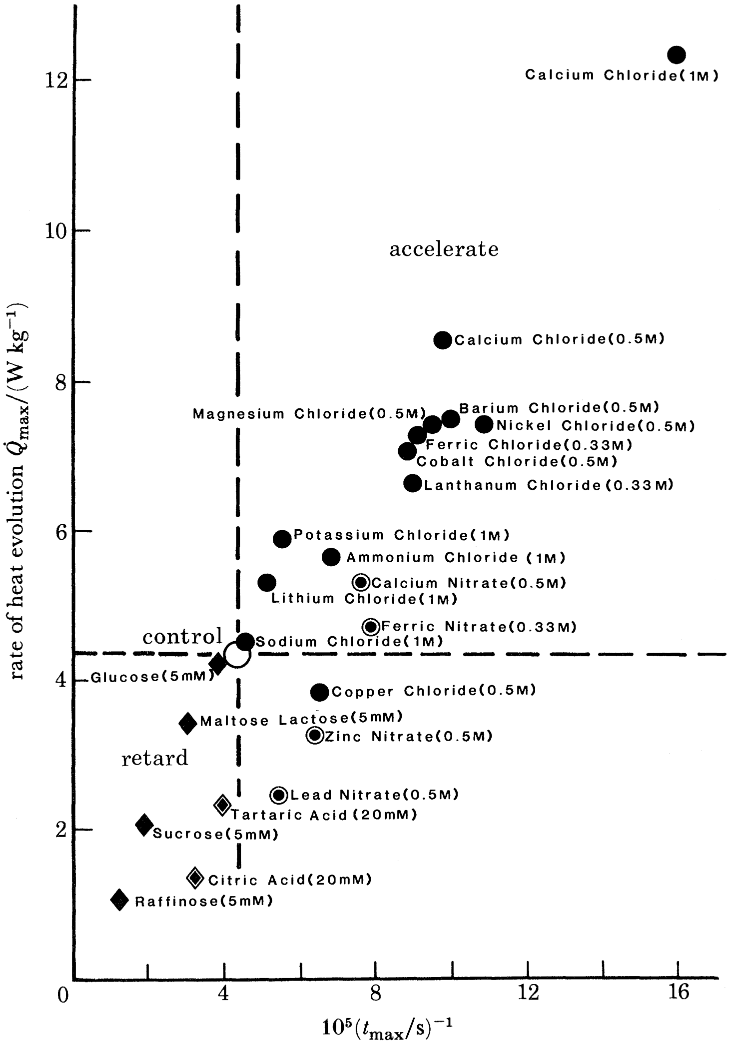

FIGURE 11. Plot of $\dot{Q}_{max}$ against $1/t_{max}$ from calorimetric heat evolution curves (see figure 6) showing the acceleration and retardation of cement hydration by a range of water soluble admixtures (w/c ratio 0.5, temperature 27 °C).

In this context, attention has been drawn to very similar growth forms, albeit on a much magnified scale, found in 'silicate gardens'. These are obtained when water soluble salt crystals with cations other than those of the alkali metals are immersed in dilute sodium silicate solution (Coatman *et al.* 1980). The analogy demonstrates very graphically the selectively permeable and osmotic characteristics of inorganic colloidal gel membranes. The effect is not confined to silicates but includes aluminates and other oxyanion species when precipitated with a metal cation as a continuous colloidal gel membrane between two solutions of differing concentrations. Figure 10*a*, *b* (plate 1) show a 'reverse' silicate garden, a sodium silicate grain immersed in a dilute solution of a calcium salt. This provides a fairly close analogy with the situation in cement. The photographs show the initial precipitation of an envelope of colloidal calcium silicate hydrate (C–S–H) gel around the dissolving silicate grain and later tubular growths developed after rupture of the coating by osmotic pressure effects.

The protective membrane model does not preclude the precipitation of hydration products within the initial gel coating. Inner products can form as the cement grains dissolve away during hydration. Since, however, the volume of hydration products exceeds that of the dissolved anhydrous material (see figure 1) not all can be accommodated in this way. Inner precipitation processes can thus be seen as an additional source of pressure within the gel coating.

6. ACCELERATING AND RETARDING ADMIXTURES

Water soluble admixtures are widely used by the industry to accelerate or retard the setting of cement. Many inorganic salts have an accelerating effect on cement hydration and the most important in commercial terms has been calcium chloride. Exceptions are Zn and Pb salts and phosphates and borates, which have a retarding effect. Commercial retarders, however, are mainly based on organic admixtures such as hydroxycarboxylic acid and sugar derivatives and these can be effective at very low concentrations.

Calorimetric methods have proved effective in classifying admixtures (Previte 1971; Kantro 1975; Kondo *et al.* 1977) but comparison of results is often difficult because of the use of different parameters to measure acceleration or retardation. The system used here is based on a plot of the maximum in the heat evolution curve ($\dot{Q}_{\max}$) against the reciprocal of the time to the peak maximum ($1/t_{\max}$). Figure 11 shows that this separates admixtures along a roughly diagonal relation according to their accelerating (top right) or retarding (bottom left) capacity relative to the untreated control cement. At the extremes, the acceleration by calcium chloride and the retardation by citric acid and raffinose are evident in this plot. The degree of acceleration or retardation depends on the concentration of the admixture.

In inorganic salt admixtures both cation and anion can be effective to varying degrees and attempts have been made to rank cations and anions separately according to their accelerating or retarding stength. For example our calorimetric system applied to cements treated with chlorides and nitrates (at equivalent concentrations of anion, 0.5 gram-ion per litre) gives approximately the following ranking sequence for cations:

$$\tfrac{1}{2}\mathrm{Ca}^{2+} > \tfrac{1}{2}\mathrm{Ni}^{2+} > \tfrac{1}{2}\mathrm{Ba}^{2+}, \tfrac{1}{2}\mathrm{Mg}^{2+} > \tfrac{1}{3}\mathrm{Fe}^{3+}, \tfrac{1}{2}\mathrm{Co}^{2+} > \tfrac{1}{3}\mathrm{La}^{3+} \gg \mathrm{NH}_4^+, \mathrm{K}^+ > \mathrm{Li}^+ > \mathrm{Cs}^+ > \mathrm{Na}^+ >$$

←acceleration

$$\tfrac{1}{2}\mathrm{Cu}^{2+} > \tfrac{1}{2}\mathrm{Zn}^{2+} > \tfrac{1}{2}\mathrm{Pb}^{2+}.$$

retardation→

Similar rankings have been found for the acceleration of the hydration of C_3S (Collepardi *et al.* 1971). For calcium salts at equivalent concentrations the work of Kantro (1975) indicates the following sequence for anions in decreasing order of acceleration of C_3S hydration:

$$\mathrm{Cl}^-, \mathrm{Br}^- > \mathrm{SCN}^- > \mathrm{I}^- > \mathrm{NO}_3^- > \mathrm{ClO}_4^-.$$

The importance of calcium in the ranking system is evident but other polyvalent cations can have similar accelerating strength at appropriate concentrations. Monovalent and alkali metal cations seem only weakly effective. Attempts have been made to correlate the accelerating capacity of ions in terms of their diffusivities (Kondo *et al.* 1977). Attempts to rationalize the

the ranking have generally been inconclusive. For cations, problems arise in establishing the configurations of the ionic species, which, in the highly alkaline (pH 12–13) environment of cement, will mostly be in a hydroxylated state (for example, $Ca(OH)^+$) in solution or will be immediately precipitated as hydroxide. As discussed by Kantro (1975), the relative solubilities of the hydroxides formed by the cations are probably an important factor. Studies of Pb and Zn salts show that retardation is associated with the immediate precipitation of dense and probably impermeable coatings of hydroxide gel around the cement grains (Thomas *et al.* 1981; Arliguie *et al.* 1982).

TABLE 1. RETARDING EFFECT OF A RANGE OF ORGANIC ADMIXTURES

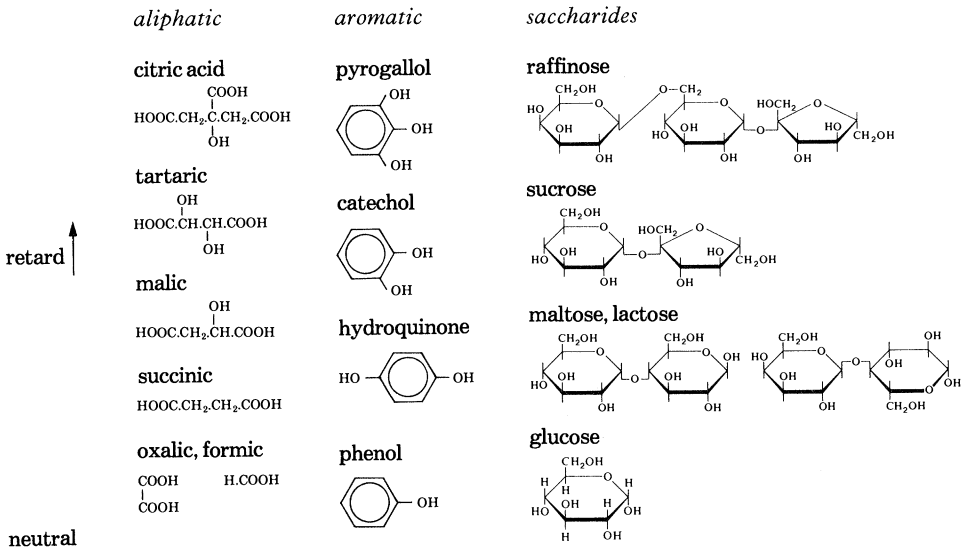

The retardation of cement by organic admixtures is primarily attributed to their effect on the hydration of the C_3S phase, but it is recognized that interactions with the aluminate phases may also be important. Explanations for the mechanism of retardation have included adsorption to the cement grain surfaces, the poisoning of nucleation and growth of the hydration products, and the precipitation of complexed species with the colloidal C–S–H gel (Young 1972). Table 1 above, based on the calorimetric ranking system, gives results for a range of aliphatic and aromatic admixtures (at 20 mM concentration) and saccharide admixtures (at 5 mM).

In the aliphatic acids there is a general increase in retardation with molecular mass and number of carboxylic groups but the important factor is the presence of α- or β-hydroxycarboxylic groups that are capable of strongly chelating a metal cation, such as calcium. In the aromatic admixtures the number and positioning of the hydroxyl groups is important and, again, this may be related to their capacity for complexing calcium. Saccharides are also capable of binding calcium (Rendleman 1966; Angyal 1980) although their chemistry in relation to cement hydration is complicated by their susceptibility to degradation by alkaline hydrolysis. The greater stability of raffinose and sucrose in this respect is significant since these are amongst the strongest retarders of cement hydration (Previte 1971). That complexation of calcium may be an important factor is demonstrated by the fact that abnormally high levels of silicon appear in solution at early stages of hydration in cements treated with EDTA, citric acid and sucrose (figure 12). Preferential sequestration of calcium by the organic molecule initially allows solubilization of the silicate, and subsequently affects the chemistry of precipitation of the C–S–H gel (Thomas & Double 1983). EDTA, which has a very strong calcium binding capability, is a relatively weak retarder compared to citric acid and sucrose. This suggests that additional factors such as the complexation of silicate (or aluminate) may also be involved, either initially as soluble complexes or finally precipitated with the C–S–H gel. Complexes of silica with citric acid and catechol are known and have been cited as the cause of promoted attack of silica glass in neutral and alkaline solutions containing dissolved organic species (Ernsberger 1959; Bacon & Raggon 1959).

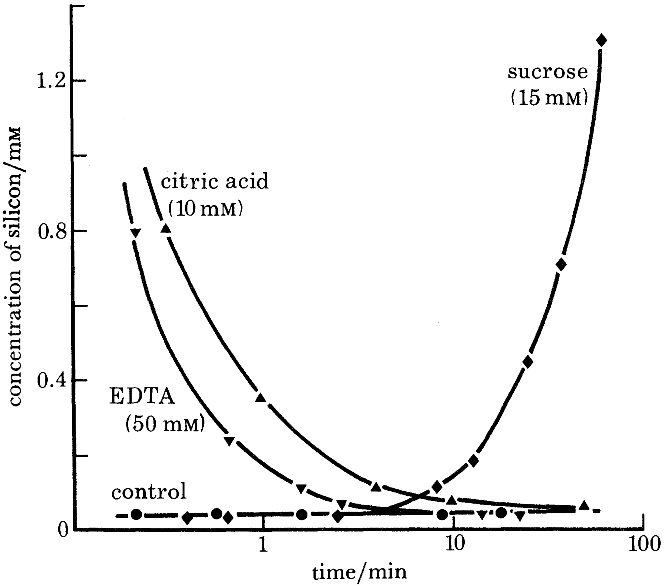

Figure 12. Concentrations of silicon in solutions filtered from cement pastes containing EDTA, citric acid and sucrose admixtures, compared with an untreated control sample (w/c ratio 2).

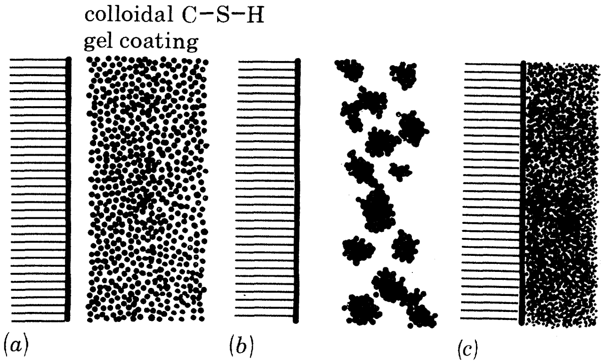

Figure 13. Schematic representation of possible changes in the colloidal structure of a C–S–H gel coating on a cement grain surface. (*a*) Normal protective gel coating, inhibiting hydration. (*b*) Flocculated, poorly adherent coating permitting accelerated hydration. (*c*) Dense, coagulated and strongly adherent coating causing retardation of hydration.

If, as seems likely, the hydration of cement is largely controlled by diffusion through protective colloidal coatings around the cement grains then it follows that the rate of reaction and the associated hydrate development will depend on the permeability and cohesion of the coatings. In these terms, cement hydration is normally self inhibiting. Modification of the colloidal coating to a more open flocculated structure will facilitate diffusion and accelerate hydration. Conversely, coagulation of the coating to a denser, less permeable and more adhesive layer will result in a retardation of hydration (figure 13).

In general, the principal cause of aggregation of a colloid is Van der Waals' attractive forces between the particles, whereas stability against aggregation is a consequence of repulsive interactions between similarly charged electrical double layers and layers arising from solvent–particle affinity. In aqueous systems, the pH of solution and dissolved salts strongly influences aggregation, and organic molecules can affect stability by adsorption on to the particle surfaces or by bridging between the particles. In this context, a tentative parallel can be drawn between the ranking of cations and anions for inorganic accelerating admixtures and the lyotropic series (Hoffmeister series), which relates to the efficacy of flocculation of hydrophilic colloids by dissolved electrolytes. Organic admixtures affect hydration by altering the chemistry of precipitation of C–S–H gel by preferential complexation of calcium or silicate in solution, or both, or by incorporation into the protective C–S–H gel coating. Measurements of ζ potentials for cement pastes show that the sign and magnitude of the electrical double layers are markedly affected in the presence of organic admixtures (Singh & Ojha 1980; Roy *et al.* 1980). Colloidal phenomena are important considerations in cement chemistry and clearly this is an area of research that will see further development in the future (Ottewill, this symposium).

The author, who is a Warren Research Fellow of the Royal Society, expresses appreciation for support from the Science and Engineering Research Council, from Imperial Chemical Industries p.l.c. and from Cormix Ltd in the development of this research. Thanks are due also to Professor Sir Peter Hirsch, F.R.S., for his encouragement, and to researchers at the Department of Metallurgy and Science of Materials at the University of Oxford, who have contributed to this work.

REFERENCES

Aldous, R. T. H. 1983 *Cem. Concr. Res.* **13**, 89–96.

Allen, A. J., Windsor, C. G., Rainey, V., Pearson, D., Alford, N. McN. & Double, D. D. 1982 *J. Phys.* D **15**, 1817–1833.

Angyal, S. J. 1980 *Chem. Soc. Rev.* **4**, 9–18.

Arliguie, G., Ollivier, J. P. & Grandet, J. 1982 *Cem. Concr. Res.* **12**, 798–6.

Bacon, F. R. & Raggon, F. C. 1959 *J. Am. ceram. Soc.* **42**, 199–205.

Bailey, J. E. & Chescoe, D. 1979 *Proc. Br. ceram. Soc.* **28**, 165–177.

Barret, P. & Ménétrier, D. 1980 *Cem. Concr. Res.* **10**, 521–529.

Birchall, J. D., Howard, A. J. & Bailey, J. E. 1978 *Proc. R. Soc., Lond.* A **360**, 445–453.

Birchall, J. D., Howard, A. J. & Double, D. D. 1980 *Cem. Concr. Res.* **10**, 145–155.

Brunauer, S., Mikhail, R. S. & Bodor, E. 1967 *J. Colloid Interface Sci.* **24**, 451–460.

Coatman, R. D., Thomas, N. L. & Double, D. D. 1980 *J. Mater. Sci.* **15**, 2017–2026.

Collepardi, M. & Marchese, B. 1972 *Cem. Concr. Res.* **2**, 57–65.

Daimon, M., Ueda, S. & Kondo, R. 1971 *Cem. Concr. Res.* **1**, 391–401.

de Jong, J. G. M., Stein, H. M. & Stevels, J. M. 1967 *J. appl. Chem., Lond.* **17**, 246–255.

Dent Glasser, L. S., Lachowski, E. E., Mohan, K. & Taylor, H. F. W. 1978 *Cem. Concr. Res.* **8**, 733–743.

Diamond, S. 1971 *Cem. Concr. Res.* **1**, 531–545.

Diamond, S. 1976 In *Proc. Conf. Hydraulic Cement Pastes; their Structure and Properties, Sheffield*, pp. 2–30. Slough: Cement and Concrete Association

Double D. D., Hellawell, A. & Perry, S. J. 1978 *Proc. R. Soc., Lond.* A **359**, 435–451.

Double, D. D., Thomas, N. L. & Jameson, D. A. 1980 In *Proc. 7th Int. Congr. Chem. Cem., Paris*, vol. II, II.356–II.260. Paris: Éditions Septima.

Ernsberger, F. M. 1959 *J. Am. ceram. Soc.* **42**, 373–375.

Fierens, P. & Verhaegen, J. 1976 *Cem. Concr. Res.* **6**, 103–111.

Flint, E. P. & Wells, L. S. 1934 *J. Res. natn. Bur. Stand.* **12**, 751–780.

Fuji, K. & Kondo, W. 1968 In *Proc. 5th Int. Symp. Chem. Cem., Tokyo*, vol. II, paper II-93, 362–370.

Groves, G. W. 1981 *J. Mater. Sci.* **16**, 1063–1070.
Jennings, H. M. & Pratt, P. L. 1979 *Cem. Concr. Res.* **9**, 501–506.
Kantro, D. L. 1975 *A.S.T.M. J. Test. Eval.* **3**, 312–321.
Kondo, R., Daimon, M., Sakai, E. & Ushiyawa, H. 1977 *J. appl. Chem. Biotechnol.* **27**, 191–201.
Lawrence, C. D. 1966 *Highw. Res. Abstr.*, report no. 90, 378–391.
Lawrence, F. V. & Young, J. F. 1973 *Cem. Concr. Res.* **3**, 149–161.
Maycock, J. N., Skalny, J. & Kalyoncu, S. 1978 *Cem. Concr. Res.* **4**, 835–843.
Odler, I. & Dörr, H. 1979 *Cem. Concr. Res.* **9**, 277–284.
Powers, T. C. 1961 *J. Portland Cem. Ass. res. dev. Labs.* **3**, 47–56.
Previte, R. W. 1971 *Cem. Concr. Res.* **1**, 301–316.
Rendleman, J. A. 1966 *Adv. carbohyd. Chem.* **21**, 209–260.
Roy, D. M., Daimon, M. & Asaga, K. 1980 In *Proc. 7th Int. Congr. Chem. Cem., Paris*, vol. II, II.242–II.245. Paris: Éditions Septima.
Singh, N. B. & Ojha, P. N. 1980 In *Proc. 7th Int. Congr. Chem. Cem., Paris*, vol. II, II.100–II.105. Paris: Éditions Septima.
Skalny, J. P. & Young, J. F. 1980 In *Proc. 7th Int. Congr. Chem. Cem., Paris*, vol. I, II.1/3–II.1/35. Paris: Éditions Septima.
Slegers, P. A. & Rouxhet, P. G. 1977 *Cem. Concr. Res.* **7**, 31–39.
Stein, H. N. 1961 *J. appl. Chem.* **11**, 474–492.
Tadros, M. E., Skalny, J. F. & Kalyoncu, R. S. 1976 *J. Am. ceram. Soc.* **59**, 344–351.
Taylor, H. F. W. & Roy, D. M. 1980 In *Proc. 7th Int. Congr. Chem. Cem., Paris*, vol. I, II.2/1–II.2/12. Paris: Éditions Septima.
Tenoutasse, N. 1969 *Report Cembureau Colloquy, Paris*, 1–16.
Thomas, N. L. & Double, D. D. 1981 *Cem. Concr. Res.* **11**, 675–687.
Thomas, N. L. & Double, D. D. 1983 *Cem. Conr. Res.* **13**, 391–400.
Thomas, N. L., Jameson, D. A. & Double, D. D. 1981 *Cem. Concr. Res.* **11**, 143–153.
Williamson, R. B. 1972 *Prog. Mater. Sci.* **15**, 3–285.
Winslow, D. N. & Diamond, S. 1974 *J. Am. ceram. Soc.* **57**, 193–197.
Young, J. F. 1972 *Cem. Concr. Res.* **2**, 415–433.
Young, J. F., Tong, H. S. & Berger, R. L. 1977 *J. Am. ceram. Soc.* **60**, 193–200.

Discussion

P. C. Hewlett (*Cementation Research Ltd, Maple Cross, Denham Way, Rickmansworth, Herts, U.K.*). Would Dr Double care to comment on the reactions taking place under the *first* hydration peak and how they take part in a recombination reaction to form the C–S–H layer on the clinker grain?

D. D. Double. A substantial proportion of the heat in the first peak derives from the heat of wetting of the cement powder and the hydration of any free lime. These tend to mask contributions from the initial hydration of the cement phases so it is difficult to arrive at any firm conclusions regarding early hydration reactions.

K. S. W. Sing (*Department of Chemistry, Brunel University, Uxbridge, U.K.*). Our work has indicated that hydrated calcium ions are only partially desolvated when they are incorporated into freshly formed C–S–H gel. Water ligands are progressively removed during the localized development of gel structure. In our view the retention and removal of this ligand water plays a key role in this hydration process and the development of gel strength. Such an approach could help to explain some of the results presented by Dr Double.

D. D. Double. It is certainly true that desolvation effects are an important factor in the agglomeration of colloidal gels, and Profesor Sing's observations are very pertinent to considerations of cement chemistry.

J. F. Raffle (*University of Technology, Loughborough, U.K.*). Dr Double classified accelerators and retarders in terms of $\dot{Q}_{\text{max}}/t_{\text{max}}$. What happens to the width of this broad peak with different accelerators and retarders?

D. D. Double. Admixtures affect the heat evolution profiles in different ways. Generally, accelerators sharpen the second peak, increase the height of the peak maximum and bring it to shorter time intervals. Retarders depress and broaden the peak so that the integrated area under the heat curve, which gives a measure of the degree of reaction, is reduced.

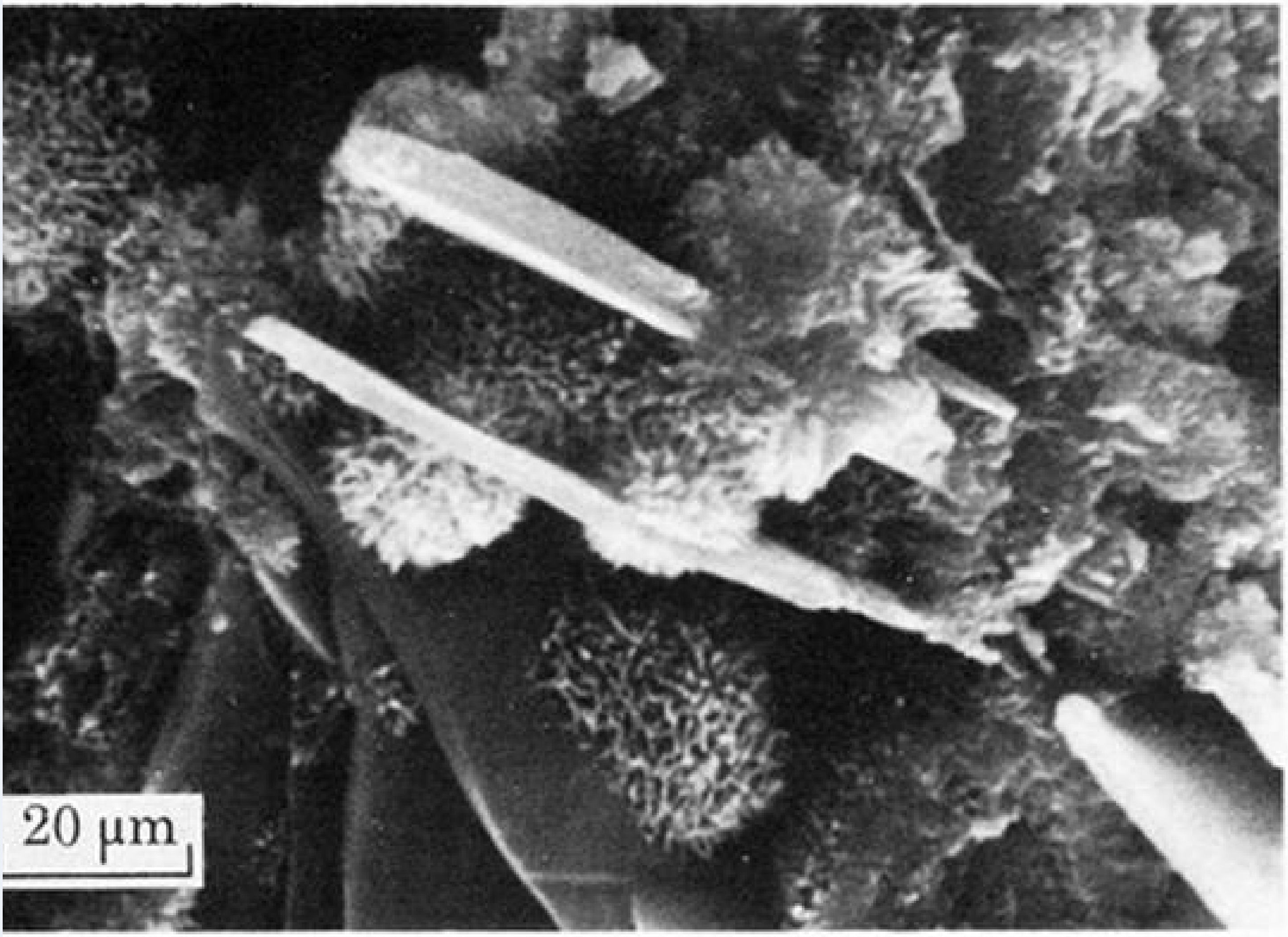

IGURE 2. Fracture surface of a hardened cement paste showing fibrillar growth of C–S–H gel around the cement grains and plate-like crystals of calcium hydroxide (w/c ratio 0.7, age 40 days). Scanning electron micrograph.

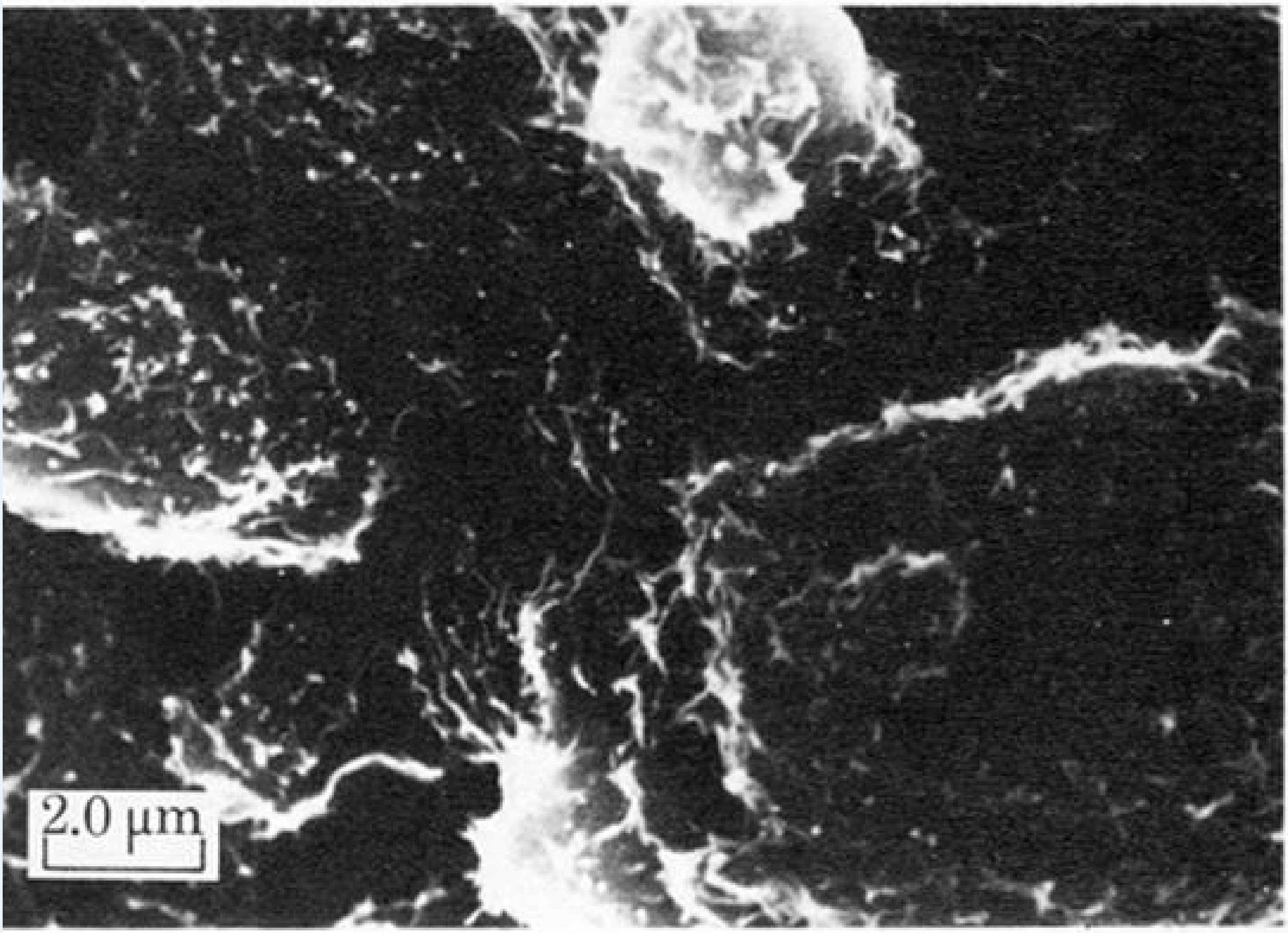

IGURE 3. Fracture surface of a C_3S paste sample at early stages of hydration showing gel coatings around the particles and the beginning of the growth of fibrillar C–S–H gel product (w/c ratio 0.5, age 2 h). Scanning electron micrograph.

PHILOSOPHICAL TRANSACTIONS OF THE ROYAL SOCIETY

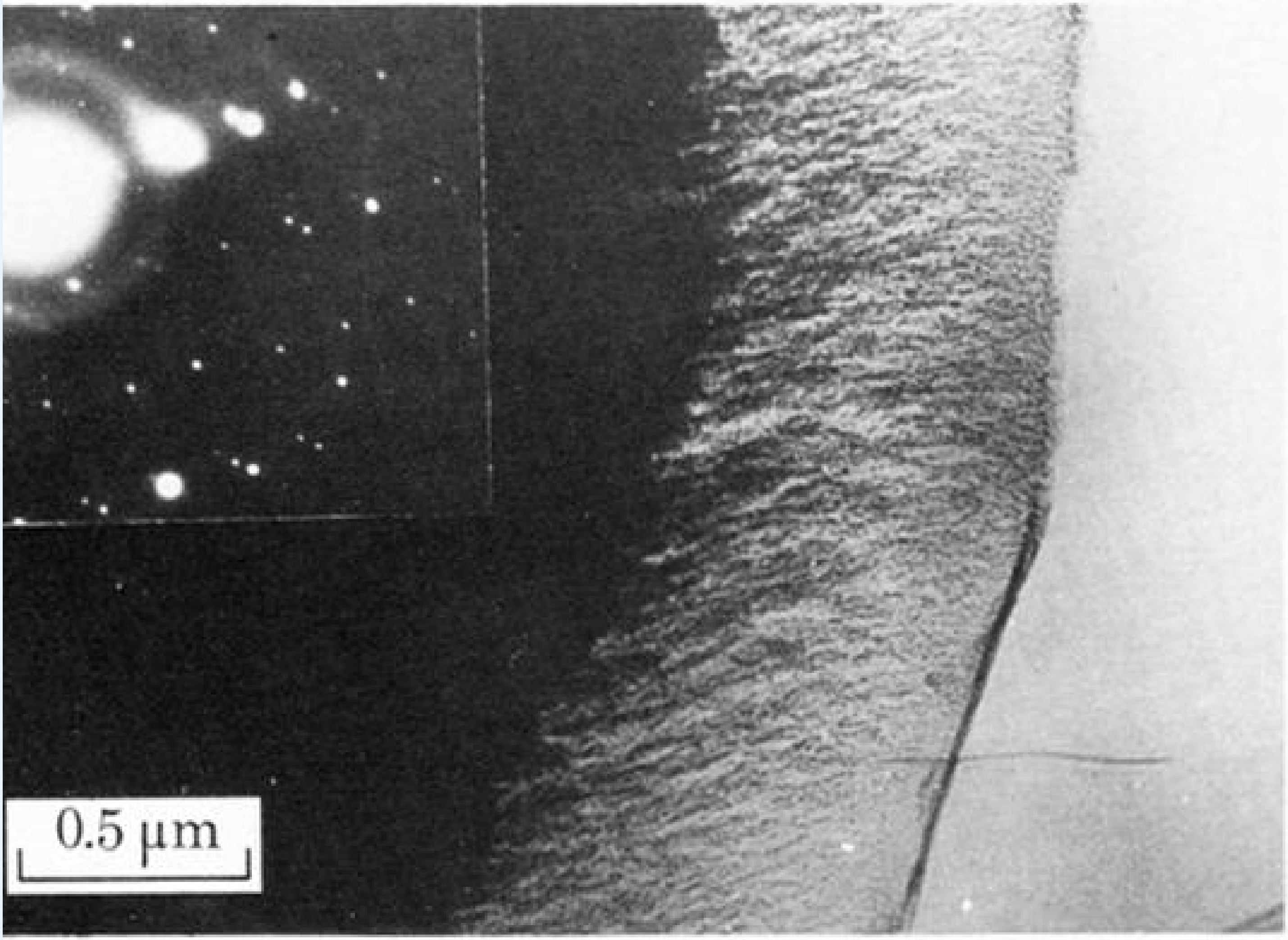

IGURE 4. Colloidal gel coating formed on a grain of C_3S in a thinned slice of Portland cement clinker after dipping in water for 5 min. Transmission electron micrograph and selected area diffraction pattern (Groves 1981).

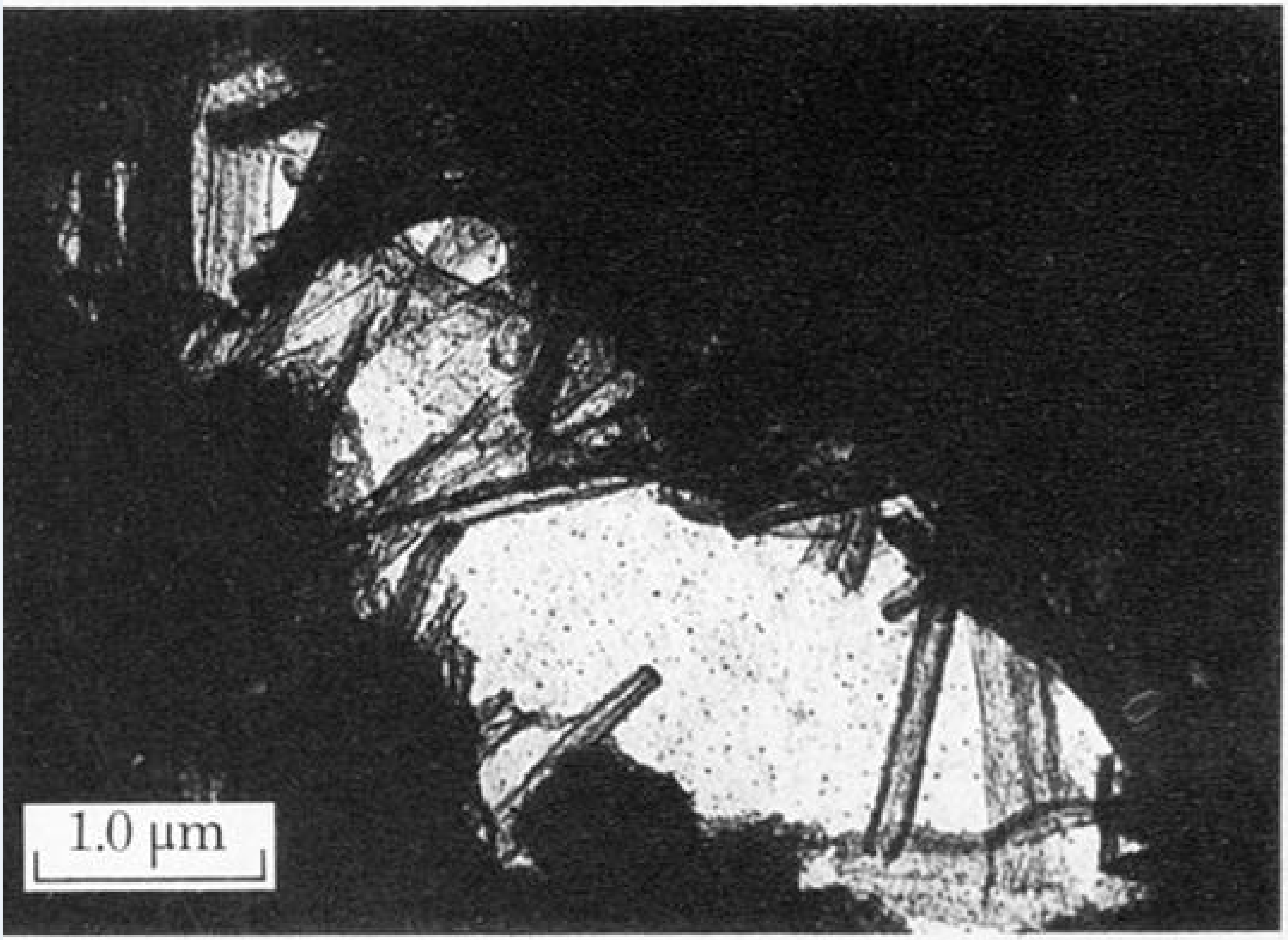

IGURE 5. Secondary growth of C–S–H gel at the surfaces of cement grains after hydration for 21 h, the hydrate shows fibrillar and crumpled sheet type morphologies. Transmission electron micrograph.

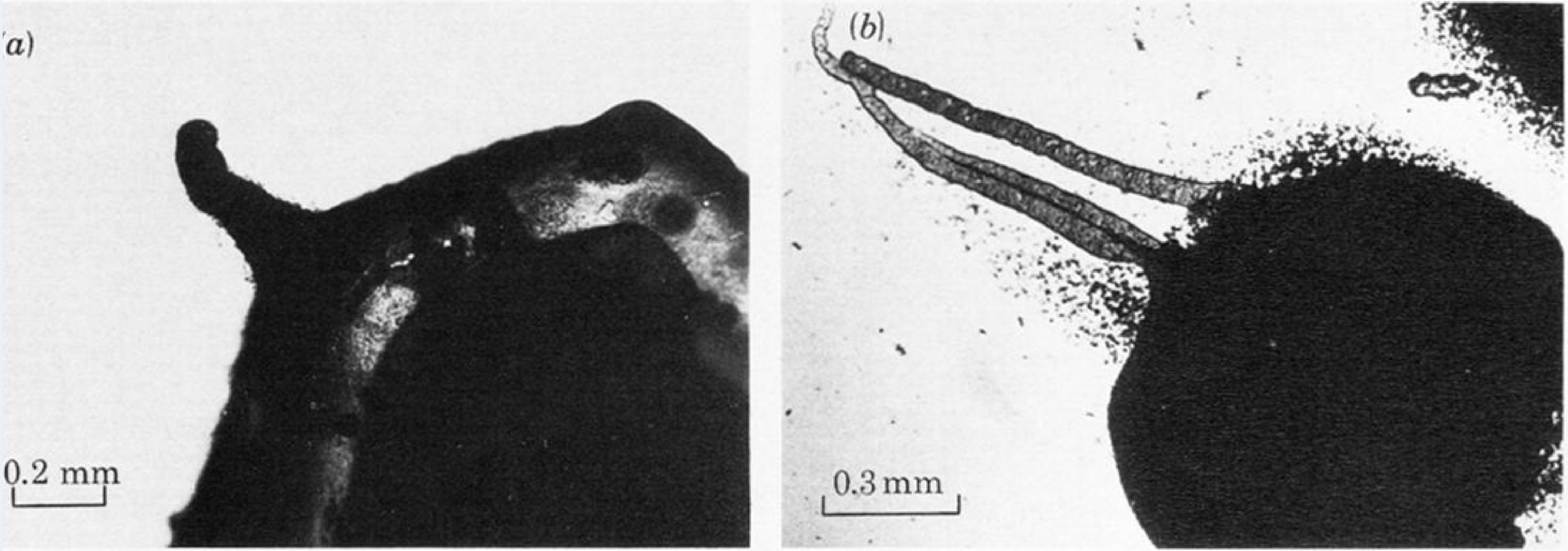

IGURE 10. 'Silicate garden' obtained by immersing a grain of sodium silicate in dilute aqueous calcium nitrate solution. (*a*) Formation of colloidal C–S–H gel coating around the dissolving grain. (*b*) Tubular growths formed after osmotic rupture of the gel coating. Optical micrographs.